Contents lists available at ScienceDirect

Arabian Journal of Chemistry

journal homepage: www.ksu.edu.sa

Integrated network pharmacology, metabolomics, transcriptomics and microbiome strategies to reveal the mechanism of Sang Ju Yin on the treatment of acute lung injury on the gut-microbiota-lung axis

Song Lin [a], Ruinan Ren [b], Fang Wang [b], Zilong He [b], Cuiyan Han [b], Jinling Zhang [c], Wenbao Wang [b], Jie Zhang [b], Huiyu Wang [b], Huimin Sui [b], Tianyang Wang [b,*]

[a] Department of Scientific Research, Basic Medical Science College, Qiqihar Medical University, Qiqihar, Heilongjiang Province 161006, China
[b] School of Pharmacy, Qiqihar Medical University, Qiqihar, Heilongjiang Province 161006, China
[c] Research Institute of Medicine & Pharmacy, Qiqihar Medical University, Qiqihar, Heilongjiang Province 161006, China

ARTICLE INFO

Keywords:
UFLC-ESI-QTOF-MS chemical component analysis
Transcriptomics
Intestinal flora
Acute lung injury
Sang Ju Yin
Metabolomics

ABSTRACT

Acute lung injury (ALI) is a clinically prevalent inflammatory disorder that still needs to be developed with more accurate diagnostic biomarkers and more satisfactory therapies. This study intended to explore the therapeutic material basis and molecular mechanisms of a classical traditional Chinese medicinal prescription, Sang Ju Yin (SJY), against ALI, focusing on the chemical components of formula composition, the disturbance of host genes/metabolites and the dysbiosis of intestinal flora. First, based on liquid chromatography-mass spectrometry (LC-MS) component analysis, 212 *in vitro* and 44 *in vivo* compounds were identified respectively in SJY. Then, network pharmacology was adopted to calculate potential anti-ALI compounds in SJY and predict that CXCR2, PI3K-Akt signaling and arachidonic acid (AA) metabolism could be potential targets. Subsequently, integrative multi-omics techniques were employed to elaborate deeper systematic molecular mechanisms. Metabolomic data combining both ^{1}H NMR and LC-MS techniques illustrated that 146 pulmonary and 75 fecal biomarkers, associated with AA and other metabolisms, were recuperated by SJY's intervention. Transcriptomic analyses suggested that SJY could significantly regulate genes and signaling pathways involved with inflammation and apoptosis, such as PI3K-Akt. Further the obtained key targets (IL-10, LCAT, CXCR2 and C5) were verified by qRT-PCR and their relative compound-target interaction were validated by molecular docking. Notably, the disturbance of intestinal microbial community (such as the abundance of Lactobacillus, etc.) was detected through 16S rRNA gene sequencing, that could be effectively reshaped by SJY. Collectively, our integrated work showed SJY could regulate the crosstalk of metabolite-target-pathway-microflora along the gut-microbiota-lung axis on the whole. Noteworthy, our study provided fundamental and new insights into how molecular networks connected different types of components, genes, metabolites, microbes and potential pathways to map an endogenous functional landscape for clinical ALI diagnosis and SJY application.

1. Introduction

Acute lung injury (ALI) is an inflammatory disease with clinical symptoms of pneumonedema, inflammation and oxidative stress (OS) disorders (Wang et al., 2020; Wu et al., 2022). Heretofore, conventional treatments with wide recognition including mechanical ventilation and hormone administration were still limited by side effects. Moreover, due to the limited interpretation of ALI nosogenesis, the popularly approved diagnostic biomarkers and recognized medications are still not available in clinic. Our previous studies have shed some light on the metabolic disturbance during ALI (Wang et al., 2020). Afterwards, considering the tight interconnection of genes and metabolites, as well as their associations with microbial dysbiosis in considerable pulmonary diseases, the interpretation of the critical role of gene-metabolite-microflora in the molecular mechanisms of ALI pathogenesis is undoubtedly required for ALI treatment, however, only short chain fatty acids in plasma samples were analyzed for metabolomic analysis in related studies, other more specific endogenous objects (such as certain genes, metabolites, etc.)

* Corresponding author.
E-mail address: tanya.sunny@163.com (T. Wang).

https://doi.org/10.1016/j.arabjc.2024.105646
Received 27 November 2023; Accepted 22 January 2024
Available online 24 January 2024

and other representative biological samples (such as lung tissues and feces) were also important for the clarification of the mechanism (Chen et al., 2022; Hashimoto et al., 2022).

Nowadays, the time-honored Traditional Chinese Medicine (TCM) and the prescription from famous medical ancient books with advantages of wide indications, recurrence prevention and low medical cost, are easy to popularize and apply, and can treat both manifestation and root cause of disorders, has developed into a type of credible treatment for healing various diseases (Wang et al., 2020; Chen et al., 2022; Wu et al., 2022). Sang Ju Yin (SJY), originated from Wenbing Tiaobian (compiled by Wu Tang in the Qing Dynasty), has significant therapeutic effects on pulmonary inflammatory diseases as traditional use, such as ALI (Zhang et al., 2014, Shen, 2020). With the traditional effect of clearing lung heat, SJY has been utilized to exert ALI intervention effects in the clear published scientific study (Zhang et al., 2014). The prescription consists of 8 flavor crude drugs, for instance, *Morous alba* L. (7.5 g), *Chrysanthemum morifolium* Ramat. (3 g), *Prunus armeniaca* L. (6 g), *Forsythia suspensa* (Thunb.) Vahl (5 g), *Mentha haplocalyx* Briq. (2.5 g), *Platycodon grandiflorum* (Jacq.) A. DC. (6 g), *Glycyrrhiza uralensis* Fisch. (2.5 g) and *Phragmites communis* Trin. (6 g). However, at present, there is still a lack of relevant research on anti-ALI effects of SJY, not to mention that therapeutic molecular mechanism requires to be further deciphered. Hence, the urgent need to study anti-ALI mechanism of SJY is emerging sequentially.

Currently, the paradigm of investigating TCM as therapeutics for complicated diseases has gradually developed into a comprehensive consideration of the complex and systemic characteristics of the overall system. Consistently, the data mining depending on the combined network pharmacology and omics technologies can establish the interaction of component-target-pathway, providing candidates of drugs acting on multiple therapy targets. Network pharmacology, due to its systematic and holistic thinking mode, is consistent with the holistic view and the TCM theoretical thinking mode of syndrome differentiation and treatment. Using network pharmacology strategies to explore the pharmacological material basis and action mechanism of TCM prescription, and using a network model of "multiple components, multiple targets, and multiple pathways" to predict the active ingredient group of TCM prescription in a targeted manner can greatly improve the efficiency of the work. For instance, through network pharmacology and transcriptomics research, the anti-inflammatory components and key targets of TCM injection of Zedoary Turmeric Oil in the treatment of ALI were elucidated (Wu et al., 2022). It is thus clear that the omics strategy has become an effective research strategy for the material basis and pathological mechanism of pharmacological effects, emphasizing the integrity of research and also in line with the principle of holistic differentiation and treatment in traditional Chinese medicine. However, the complex organism system may probably be difficult to be systematically described by single omics technology unilaterally. Accordingly, it is necessary to improve research effectiveness and cost-effectiveness to deeply solve the scientific problems, and the integration of transcriptomics and metabolomics has been developed as powerful bioinformatics technologies for elucidating internal changes in genes and metabolites from the perspectives of cause and effect (Wang et al., 2022). For example, the mechanism of action of Huanglian Jiedu Decoction against ALI has been contentedly explained by combining transcriptomics and metabolomics from the unique perspective of the sphingolipid pathway and inflammasome, however, since inflammation were crucial pathological injuries of ALI, the diagnostic inflammatory endogenous metabolic profiling with more specificity and relativity, such as arachidonic acids profiling, was still required further exploration (Chen et al., 2022). In addition, gradually deepened researches have supported the pivotal role of the gut-lung axis in the mechanism illustration of diseases, especially pulmonary disorders (Wypych et al., 2019). Results of correlations between interleukin (IL) levels and several gut microbes (or metabolites from metabolomics results) have further suggested that the gut-microbiota-lung axis is intimately linked to ALI pathogenesis, in all probability even to the drug intervention (Hashimoto et al., 2022). Additionally, the immune-regulation effect of microflora such as *Lactobacillus* has been reported to produce inflammatory regulator (such as IL-10) and prevent successive tissue inflammation (Liu et al., 2022). However, whether the regulatory effects of SJY on microbial communities are consistent with the treatment of ALI with other TCM therapies is unclear, not to mention the overall regulation effects of SJY on the whole system of the gut-microbiota-lung axis.

Until now, there is still a lack of the investigation of anti-ALI effects of SJY, let alone the therapeutic compounds or action mechanism about the interaction of gene-metabolite-microflora. Therefore, this research was performed for the first time to develop a novel conjoint approach to delve into potential protective components and action mechanism of SJY based on the host-flora interaction on the gut-microbiota-lung axis, combining LC-MS component analysis, network pharmacology, metabolomics, transcriptomics and microbiomes, with the assist of verification experiments (such as qRT-PCR and molecular docking), especially further attributing to understanding the crosstalk between pivotal metabolites, targets and pathways. Collectively, the systematic strategy compensates network pharmacology for lacking experiment verification, and single-omics for lacking upstream/downstream molecular mechanisms and drug-binding targets, and researches on body system for lacking host-microflora interactions in the environment. This strategy is expected to provide new insights into the action mechanism of SJY for ALI treatment. And this work will provide more support for both promoting TCM and addressing the needs of tackling difficult clinical diseases.

2. Materials and methods

2.1. Preparation of SJY

All herbs in SJY were purchased from Tong-Ren-Tang Pharmacy (Qiqihar, China). Herbs were extracted according to the procedures of 30 min soaking, twice boiling, filtration and concentration (detailed procedures were shown in Supplementary Material).

2.2. Animals

Male rats (180–220 g, Wistar) were acquired by Qiqihar Medical University (QMU) Experimental Animal Center (Qiqihar, China), raised in a special pathogen free (SPF) standard pattern. Whole operations were granted by the Animal Ethics Committee of QMU (ethical registration number: QMU-AECC-2021-86). After acclimatization one week prior to the experiment, all animals were randomly grouped, then applied to abrosia for 12 h prior to drug administration: On the one side, considering SJY component identification *in vivo*, rats (n = 6) were gavaged with SJY (4 g/kg/d, rat dose was calculated from human dose by body surface area algorithm) for 2 weeks. The plasma was gathered then combined 2 h before and after administration every day. On the other side, animals for multi-omics studies were grouped as control, ALI (intratracheally, 5 mg/kg LPS at day 5, lipopolysaccharide, *Escherichia coli* 055:B5, Sigma Chemical Co, St. Louis, MO, USA) and SJY (4 g/kg SJY, gavage administration, day 1–5) groups (n = 8). At day 5, LPS modeling was carried out and SJY was given 2 h prior to LPS challenge. Because SJY has been a famous clinical commonly used formula recorded in Wenbing Tiaobian, the animal dosage was calculated based on the classic original recorded general human dosage from Wenbing Tiaobian using the body surface area conversion algorithm. After 6 h of modeling, all animals were executed under anesthesia to gather lungs and feces, etc.

2.3. Component analysis by UFLC-ESI-Q/TOF-MS

Both *in vitro* and *in vivo* phytochemical profile of SJY was analyzed through a UFLC-ESI-Q/TOF-MS system, mainly including the

Prominence™ UFLC XR system (LC-20 A, Shimadzu, Kyoto, Japan) and TripleTOF™ 4600 (Sciex, Foster City, CA, USA). Analytes were separated by the C_{18} column (2.1 × 100 mm, 1.7 μm, ACQUITY UPLC HSS T3, Waters, Milford, MA, USA). Both ESI^+ and ESI^- modes were adopted and the mass range of TOF MS scan was *m/z* 50–1500. Detailed information was shown in Supplementary Material.

2.4. Network pharmacology

The network of component-target-pathway about SJY against ALI was constructed as following: (1) Given the *in vitro* to *in vivo* transitivity, SJY's ingredients absorbed into blood were screened out as candidate compounds. Their related top 20 targets were calculated by SwissTargetPrediction (https://www.swisstargetprediction.ch/) to obtain Set1. (2) ALI related targets (Set2) were obtained on GeneCards (https://www.genecards.org) with DrugBank (https://www.drugbank.ca/). The intersection of Set1 and Set2 was filtered as targets about SJY against ALI. (3) The network of protein–protein interaction (PPI) was created based on STRING (https://cn.string-db.org/). (4) Enrichment analysis was achieved via Metascape (https://www.metascape.org/) ($p < 0.05$). (5) The Cytoscape 3.7.2 (Cytoscape Consortium, CA, USA) was utilized for visualization of the ingredient-target-pathway ternary network.

2.5. Anti-ALI effects of SJY

2.5.1. Histopathological analysis

The right upper lobe was rinsed with cold PBS instantly for hematoxylin and eosin (H&E) staining in order to examine histopathologically.

2.5.2. Lung wet/dry (W/D) ratio

After washing the right middle lobe of lung with cold PBS, the wet weight value (WWV) was weighed. Then, after 48 h incubation (dried at 80 °C), the dry weight value (DWV) was gained. Finally, the W/D ratio was numerated according to WWV/DWV * 100 %.

2.5.3. Inflammation and OS indices assessment

ELISA determination of inflammation cytokines (TNF-α, IL-3 and IL-6) and oxidant stress (OS) indicators (GSH, SOD and MDA) in lung tissue were accomplished according to the producer's instructions (kits for OS were cultivated from Jiancheng Bioengineering Institute of Nanjing, Jiangsu, China; the rest were purchased from MLBio Biotechnology Co., Ltd., Shanghai, China).

2.6. UFLC-ESI-QTOF-MS metabolomic profiling

2.6.1. Sample preparation

In brief, the pulmonary homogenates were prepared with methanol, and the fecal freeze-dried powders were extracted twice with ethyl acetate and methanol-deionized water (80:20, *v/v*). The final supernatants were assembled for injection. More information processing steps were recorded in Supplementary Material.

2.6.2. Chromatography and mass spectrometry conditions

Analyses were performed utilizing the Prominence™ UFLC XR system (LC-20 A, Shimadzu, Kyoto, Japan) and quadrupole time-of-flight (AB Sciex TripleTOF™ 4600). The separation was conducted through the C_{18} column (2.1 × 100 mm, 1.7 μm, ACQUITY UPLC BEH, Waters, Milford, MA, USA). The mass range of TOF MS scan was *m/z* 50–1000. Rest params were referred in Supplementary Material.

2.6.3. Data processing and metabolites identification

The metabolomic data from UFLC-ESI-QTOF-MS was further analyzed using the XCMS package of the R platform (version 4.0, Inc., Boston, USA). Pareto-scaling normalization was used for preprocessing of the data matrix. Generated data matrix was imported to SIMCA-P (version 14.0, Umetrics, Umea, Sweden) and handled by means of PLS-DA. Differential metabolites (DMs) were screened out in the light of 3 parameters (FC > 2, VIP > 1 and $p < 0.05$), then identified by comparing MS/MS spectrum and accurate mass with relevant papers and public databases, for instance, Massbank (https://www.massbank.jp), HMDB (https://www.hmdb.ca/) and mzCloud (https://www.mzcloud.org/).

2.7. ^{1}H NMR metabolomic profiling

2.7.1. Sample preparation

Basically consistent with the metabolomics preparation method until the reconstitution step, that 300 μL phosphate buffer (pH 7.0) and 300 μL phosphate buffer (pH 7.0) prepared with of deuterium oxide (D_2O, 99.9 %, containing 0.05 % 3-(trimethylsilyl)propionic-2,2,3,3-d4 acid sodium salt, Sigma-Aldrich, Dorset, U.K.) were added. After vortexing for 3 min and centrifuging for 10 min (12,000 rpm and 4 °C), the upper layer of the mixture was collected for analysis.

2.7.2. ^{1}H NMR spectrum acquisition

Metabolomic profiling was conducted using proton Nuclear Magnetic Resonance (^{1}H NMR). NMR spectra were acquired at 298 K for each sample at 500 MHz on a Bruker spectrometer (Bruker BioSpin, Karlsruhe, Germany) using the Carr-Purcell-Meiboom-Gill (CPMG) sequence to restrain the signal of protein.

Within the spectral width of 7,500 Hz, ^{1}H NMR spectra were recorded with 128 scans into 32 K data points. Zero-filled consequential free induction decays (FID) were multiplied by the exponential line broadening function with a 0.5 Hz line broadening factor prior to Fourier transform.

2.7.3. Data processing and metabolites identification

By means of operations such as baseline correction, peak comparison normalization, metabolite identification, the ^{1}H NMR information was processed by ASICS package of R platform, meanwhile, 4.5–5.1 ppm water related part was blocked. The PLS-DA analysis was conducted with global metabolic matrix via SIMCA-P. DMs with VIP > 1 and $p < 0.05$ were further selected.

2.7.4. Metabolomic biomarkers analysis

Metabolomic biomarkers were uploaded to MetaboAnalyst (https://www.metabo-analyst.ca/) and R platform to analyze a comprehensive survey of the metabolic pathways with the significance threshold setting as $p < 0.05$.

2.8. Transcriptomic profiling

2.8.1. RNA extraction, library construction, and sequencing

Rat lung samples from the control, ALI, and SJY groups (n = 5) were sent to Shanghai Bioprofile Technology CO., Ltd (Shanghai, China). After RNA extraction, purification and library construction, Agilent 2100 Bioanalyzer (Agilent Technologies Co. Ltd., USA) was used to inspect the library. The samples were sequenced using the next-generation sequencing (NGS) technology, based on the Illumina Novaseq 6000 platform, and the paired-end (PE) sequencing of the library was performed.

2.8.2. Data processing and DEGs identification

Gene expression profiles were analyzed via the limma package of R platform. Finally, the differential analysis of assembled and quantified genes was conducted in line with $p < 0.05$ and $|\log_2 FC| > 0.5$ to screen out differentially expressed genes (DEGs).

2.8.3. Function enrichment analysis of DEGs

For the sake of perceiving the bio-significance of DEGs, the

Metascape platform (https://metascape.org) was adopted for enrichment analysis. KEGG annotation was performed with other parameters presumed as default settings. Significantly enriched terms of adjusted $p < 0.05$ were acquired on the basis of Hypergeometric test and Benjamini-Hochberg adjusted p-value correction algorithm. The enrichment analysis results were displayed by R platform.

2.9. Verification of key targets by molecular docking and qRT-PCR

The key targets screened by the intersection data of RNA sequencing and network pharmacology were selected as key targets (e.g., IL-10, LCAT, CXCR2 and C5), then validated by qRT-PCR (the $2^{-\Delta\Delta Ct}$ method was used to assess the relative RNA expression levels, primers and results were shown in Supplementary Material). Additionally, these key targets were selected as receptors, and the concerned components from network pharmacology were selected as ligands. Next, the highly automatic protein–ligand blind docking was conducted by means of CB-Dock2 with default parameters (shown in Supplementary Material).

2.10. DNA extraction and 16S rRNA gene sequencing

Library establishment and Illumina sequencing were proceeded by Shanghai Bioprofile Technology CO., Ltd (Shanghai, China). The total genomic DNA from gut microbiota in fecal samples was extracted, then verified by 1.2 % agarose gel electrophoresis, and DNA concentrations were determined using NanoDrop spectrophotometry. All samples were quantified on a Microplate reader (BioTek, FLx800, USA). The V3-V4 hypervariable region of the 16S rRNA gene was amplified using barcoded primers (forward primer: 338F (5′-ACTCCTACGGGAGGCAGCA-3′); reverse primer: 806R (5′-GGACTACHVGGGTWTCTAAT-3′)) and sequenced via the Illumina NovaSeqPE250 platform. The amplicons from different samples were pooled, purified and sequenced. The microbial sequence data were analyzed using QIIME 2 (version 2019.4) and R package.

2.11. Statistical analysis

Calculations about statistical analyses and integrative analysis of multi-omics information was conducted on the basis of R platform.

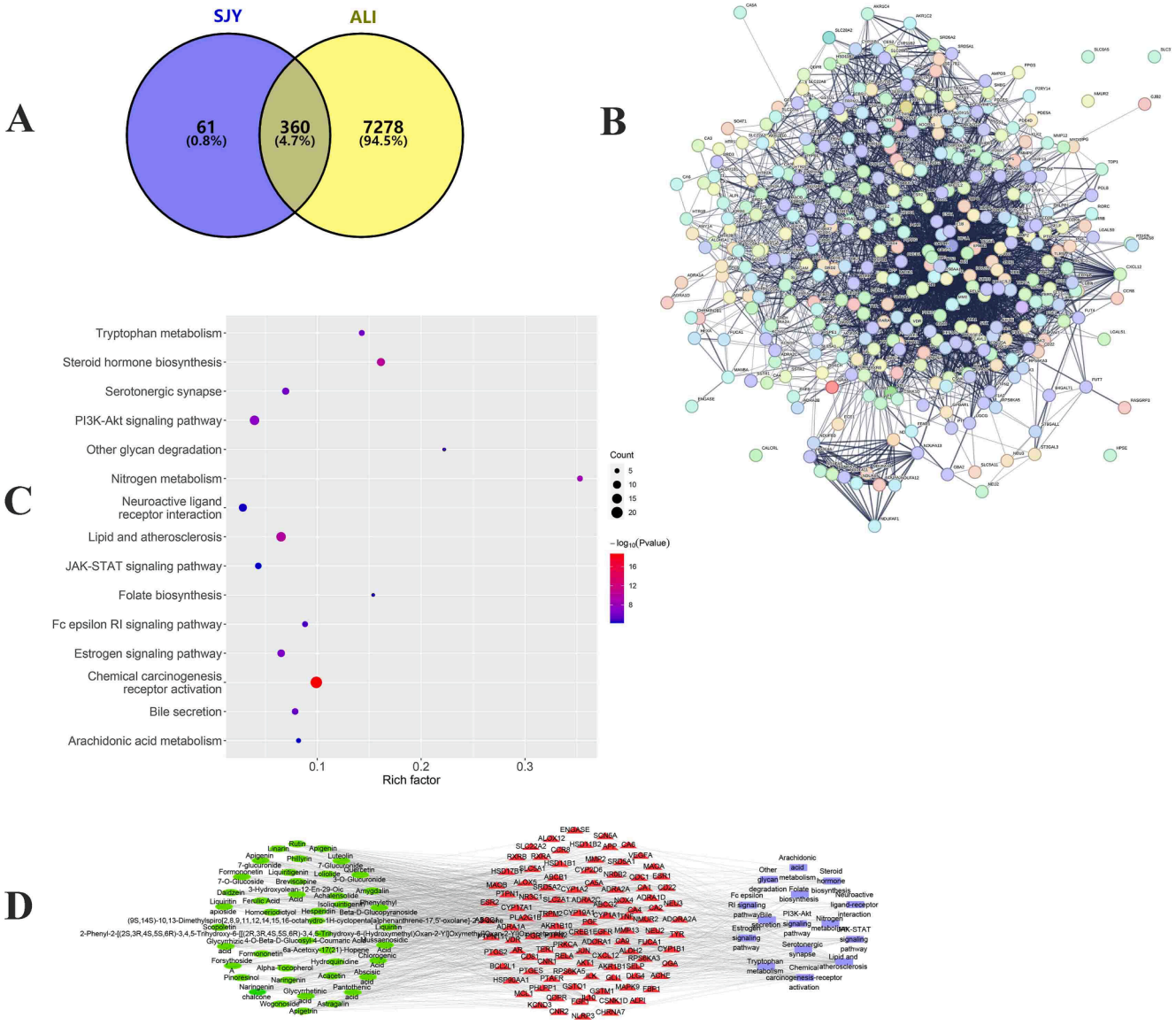

Fig. 1. Network pharmacology uncovers the mechanism of SJY for ALI. (A) Venn diagram of targets shared by SJY and ALI; (B) PPI network based on targets of SJY for ALI; (C) Representative terms in enrichment analysis; (D) The component-target-pathway network construction about anti-ALI of SJY.

Lilikoi package and GSVA package was used to evaluate the quantitative changes of pathways for metabolomics and transcriptomics, respectively. All experimental data were expressed using Mean ± SD, and inter-group differences were explored by Student's *t*-test. The results satisfying $p < 0.05$ were given statistical significance.

3. Results

3.1. Construction of the component-target-pathway ternary network in view of SJY component analysis

On account of the LC-MS/MS method established in our study, compounds in SJY were effectively identified. Eventually, a chemical composition database of SJY (containing 212 *in vitro* compounds) was constructed, of which 44 compounds were absorbed into the blood, which preliminarily clarified the chemical basis of SJY (Table S2). Next, network pharmacology was further adopted, and a multivariate database was established, among which, 44 potential active ingredients were filtered regarding *in vivo* effects of SJY, meanwhile, 105 targets and 15 pathways were involved. Considering this ternary network, intervention effects of multi-components in SJY (such as rutin, chlorogenic acid, amygdalin, phillyrin, naringenin, acacetin and liquiritin, etc.) were involved with ALI pathogenesis through multi-targets (such as IL-10, LCAT, CXCR2, C5, etc.), and multi-pathways (such as PI3K-Akt, JAK/STAT signalings and metabolisms especially AAs, steroids and lipids), etc. (Fig. 1). The above results illustrated the potential intervention mechanism of SJY against ALI, and also provided the potential pharmacological substances.

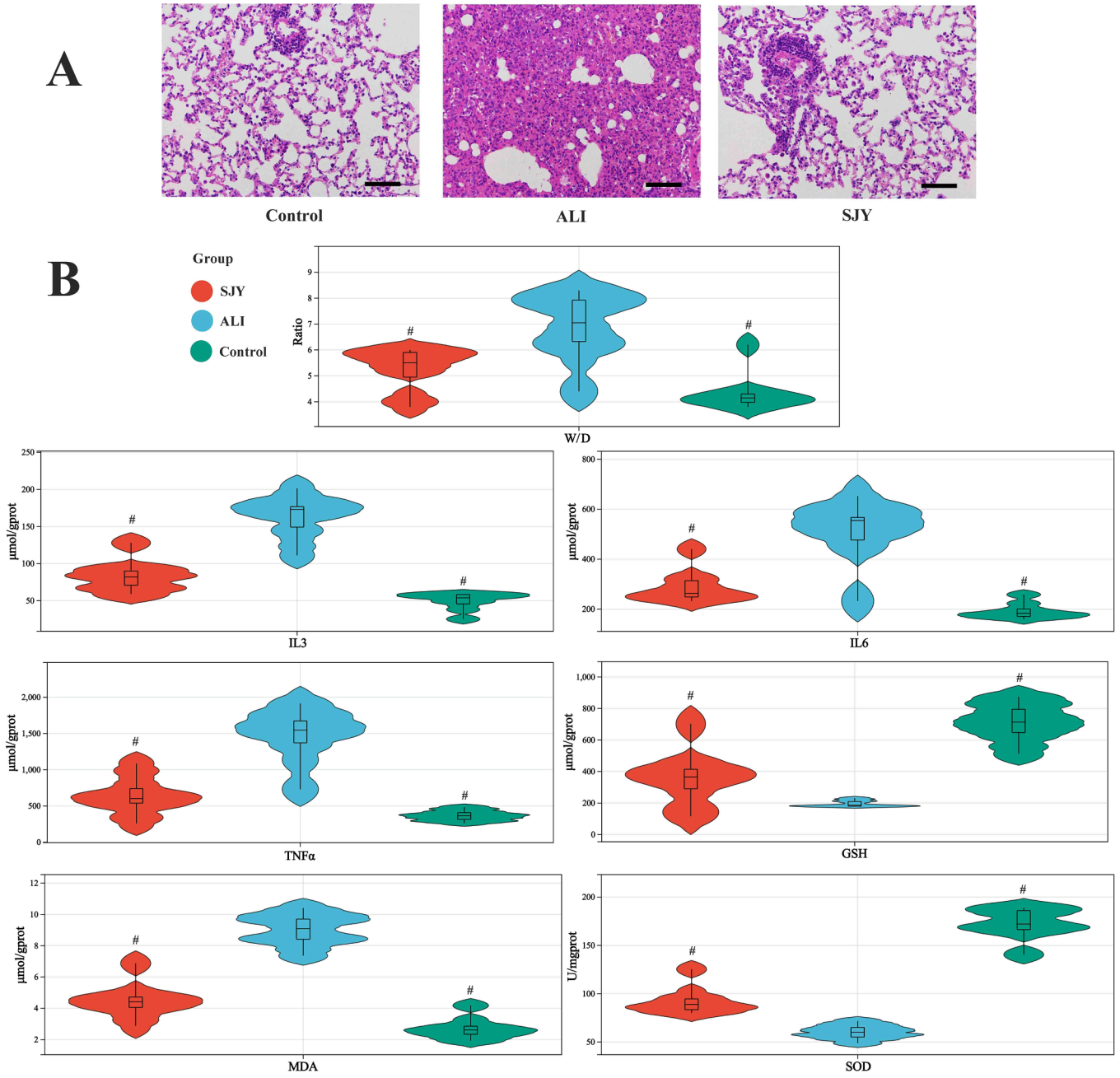

Fig. 2. Pathological and biochemical assessment of intervention effects of SJY on ALI: (A) H&E staining (×200 magnification); (B) Lung W/D ratio and ELISA results of IL-3, IL-6, TNF-α, GSH, MDA and SOD in lung sample. #: Significant difference compared with model group ($p < 0.05$).

3.2. The intervention effects of SJY on ALI

The symptoms of ALI (respiratory distress and hair gloss), pathological indicators (H&E staining, lung W/D ratio, white blood cell (WBC) count in BALF and protein concentration assay in BALF, etc.) and biochemical indicators (IL-3, IL-6, TNF-α, SOD, MDA and GSH, etc.) were used as evaluation indicators to investigate the anti-ALI effects of SJY. Pathological indexes of rats in each group were compared (Fig. 2 and Fig. S3). The results showed that after LPS treatment, typical ALI symptoms such as decreased activity and shortness of breath were observed in model rats. Extensive interstitial hydroncus, broaden alveolar septa and inflammatory cells infiltration were shown in lung tissue sections of rats, and various inflammatory and oxidation-related indicators were significantly abnormal, suggesting that the ALI model was successfully established. On the one hand, the levels of TNF-α, IL-3, IL-6 and MDA in ALI model group displayed a remarkable increase compared with control group. Additionally, the levels of GSH and SOD in lung homogenates of ALI rats was significantly decreased compared to control group. While, after drug treatment, results showed that SJY could significantly improve abovementioned pathological symptoms.

3.3. The intervention effects of SJY on ALI in respect of characteristic metabolites

3.3.1. Metabolomic analysis by UFLC-ESI-QTOF-MS

First, to prove the method reliability, the method was validated in respect of instrumental precision, repeatability and stability by inserting QC samples into injection sequence (Supplementary Material). For both lung and feces samples, the score plots of PLS-DA model (both ESI^+ and ESI^- modes) presented the holistic views of the metabolome profiles. The noticeable separate clusters of distinct groups were obtained in PLS-DA results, and satisfactory results were observed from the permutation tests (Fig. 3). The overall 124 and 53 different forms of DMs were identified with significant variations in lung and feces, respectively (Table S5). Detailly, most metabolites were restored after SJY administration, suggesting that SJY treatment could ameliorate the metabolic perturbations during ALI.

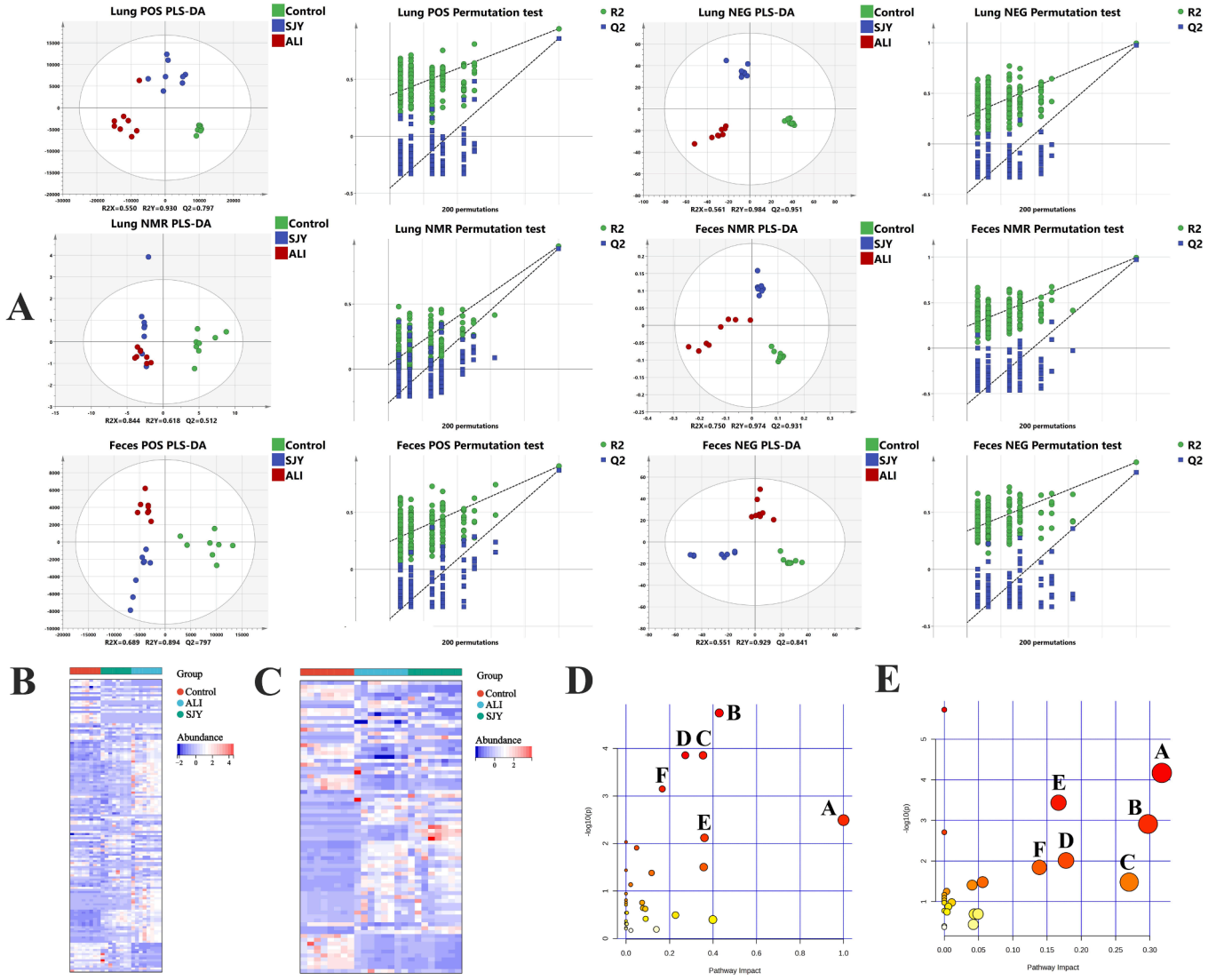

Fig. 3. Metabolomic analysis. (A)The PLS-DA score plot and permutation test of lung and feces samples in UFLC-ESI-QTOF-MS and ^{1}H NMR metabolomics among Control, ALI and SJY group; Heatmap of the differential metabolites (B) in lung and (C) in feces; (D) Pathways analysis of metabolites regulated by SJY in lung; ((D-A) Phenylalanine, tyrosine and tryptophan biosynthesis; (D-B) Taurine and hypotaurine metabolism; (D-C) Arachidonic acid metabolism; (D-D) Glycerophospholipid metabolism; (D-E) Glycine, serine and threonine metabolism; (D-F) Aminoacyl-tRNA biosynthesis.) (E) Pathways analysis of metabolites regulated by SJY in feces. ((E-A) Glycine, serine and threonine metabolism; (E-B) Glycerophospholipid metabolism; (E-C) Sphingolipid metabolism; (E-D) Cysteine and methionine metabolism; (E-E) Aminoacyl-tRNA biosynthesis; (E-F) Arginine and proline metabolism.)

3.3.2. Metabolomic analysis by ^{1}H NMR

A total of 44 different forms of DMs (For example, Taurine in lung was identified by 3.3 (t) & 3.4 (t), and Valine in feces was identified by 1.1 (d) & 3.6 (d)) were identified with obvious differences in lung and feces respectively by ASICS algorithm analysis (Table S5), thereinto, most of which could be backward adjusted by SJY intervention, implying satisfactory effects of SJY on ALI. Quite like UFLC-ESI-QTOF-MS metabolomics, combined PLS-DA model and permutation test was utilized for ^{1}H NMR data, unveiling the callback capability of SJY on endogenous chaos (Fig. 3).

3.3.3. Pathway analysis of metabolomic biomarkers

The pathway enrichment analyses for all DMs in lung and feces were carried out on MetaboAnalyst. Regarding metabolomic pathway analysis in lung regulated by SJY, phenylalanine, tyrosine and tryptophan biosynthesis, taurine and hypotaurine metabolism, arachidonic acid (AA) metabolism, glycerophospholipid metabolism, etc. were the most significant metabolic pathways (Fig. 3). Meanwhile, the variations of glycine, serine and threonine metabolism, glycerophospholipid metabolism, sphingolipid metabolism, etc. caused by ALI were evidently intervened by SJY in feces (Fig. 3).

3.4. The intervention effects of SJY on ALI in respect of on differential expressed genes

The comparison of gene expression levels was carried out between ALI group with control group and SJY group respectively. Finally, a total of 263 DEGs (intervened by SJY) were recommended by the intersection of DEGs between control with ALI groups and DEGs between ALI with SJY groups (Fig. 4 and Table S6). Further, KEGG enrichment analysis results explicated that SJY-intervened-DEGs were involved significantly in biological pathways including PI3K-Akt, NOD-like receptor signaling pathway and viral protein interaction with cytokine and cytokine receptor, etc. (Fig. 4).

To obtain an in-depth view of the intervention mechanism of SJY on ALI, the 4 key targets (LCAT, IL-10, CXCR2 and C5) were screened out via an intersection of network pharmacology and RNA-seq. To further validate the intervention of SJY and these targets, the molecular docking between targets and concerned components in SJY (e.g., rutin, chlorogenic acid, amygdalin, phillyrin, naringenin, acacetin, liquiritin, etc.) were carried out. Results showed that all the compound-target pairs with binding energy values ranged from −10.1 kcal/mol to −6.4 kcal/mol were attributed to higher binding affinities (Table S7). On the other hand, the qRT-PCR results of the key targets were comparatively in accordance with the expression of DEGs in RNA-sequencing (Fig. S4). Together, these data verified the intervention role of SJY's components on ALI in respect of key targets.

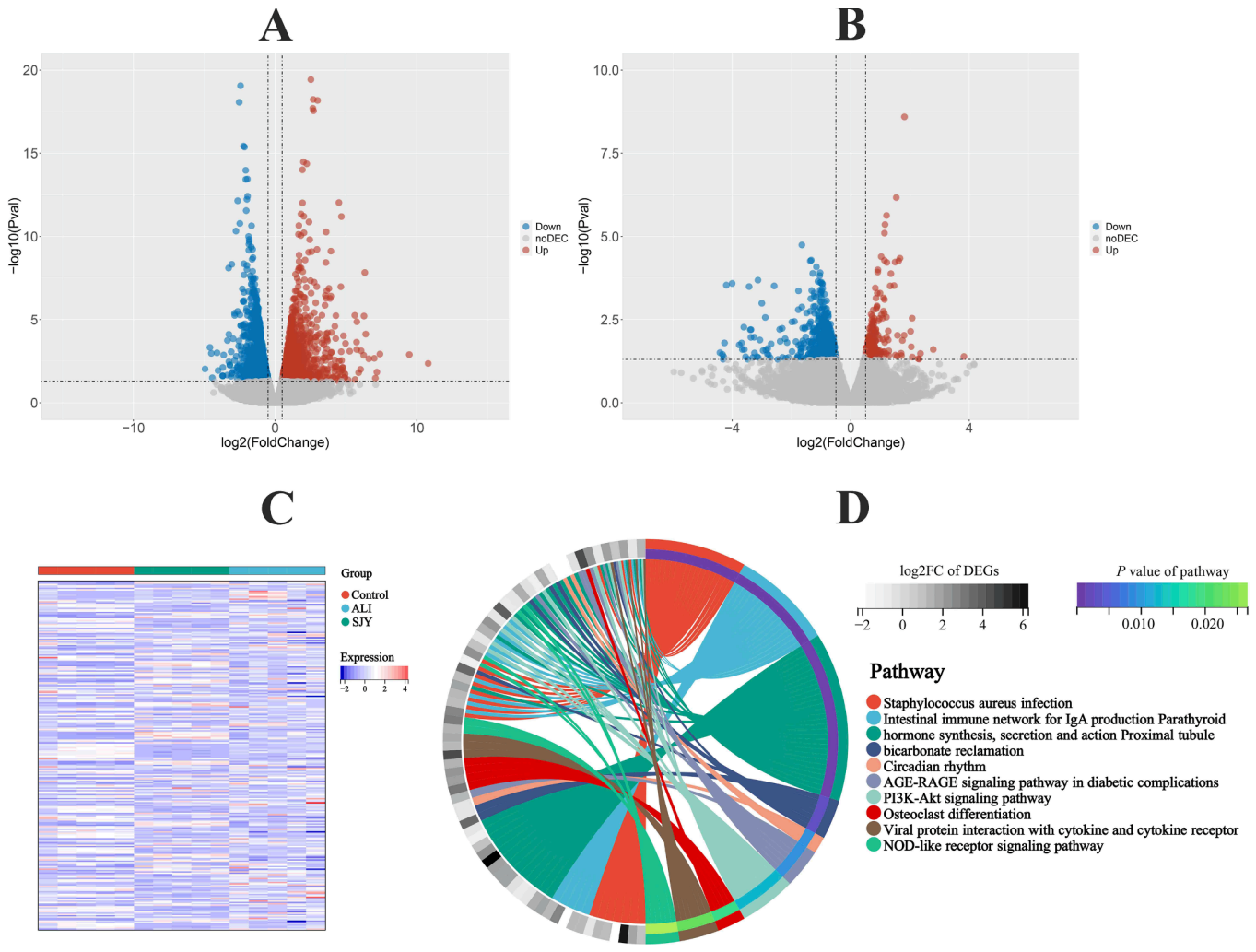

Fig. 4. SJY regulates the expression of genes related to ALI. Volcano plot results of limma algorithm for (A) ALI group *vs* Control group and (B) SJY group *vs* ALI group; (C) Heatmap for hierarchical cluster analysis of DEGs in different groups; (D) KEGG enrichment analysis of DGEs significantly intervened by SJY.

3.5. The effects of SJY on the intestinal flora structure

The regulatory role of SJY on gut microbiota was obtained by the 16S rRNA gene sequencing results (Table S8). To assess the diversity differences between different groups, β-diversity analysis was adopted. A distinct clustering of microbiota composition for control, ALI, and SJY groups using UniFrac-based principal coordinates analysis (PCoA) was acquired, suggesting the core microbiota changed evidently after SJY intervention (Fig. 5A). To further visualize differences in the taxa of the gut microflora among different groups, NMDS analysis was carried out, showing a prominent variation of microbiota composition in ALI group (Fig. 5A). On the other hand, the community function diversity of ALI group was lower on account of Shannon and Simpson indexes (Fig. 5A). Besides, the abundances of representative microbiota were significantly altered in various hierarchical orders, for instance, at the genus level, *Dubosiella* and *Allobaculum*, etc. raised prominently compared with control and SJY groups; *Lachnospiraceae*_NK4A136_group and *Ruminococcaceae*_UCG-005, etc. decreased sensibly compared with control and SJY groups (Fig. 5B). Additionally, in order to discover characteristic microflora at each taxonomic level, linear discriminant analysis (LDA) and LDA effect size (LEfSe) were utilized to further appraise the abundance of differential taxa, and a cladogram was shown in Fig. 5C. For SJY intervention, the class *Bacilli*, order *Lactobaccillales*, family *Lactobaccillaceae* and genus *Lactobacillus*, etc. could be identified with sensitivity for SJY against ALI (Fig. 5).

3.6. Integrative analysis of multi-omics on the gut-microbiota-lung axis

On account of the multi-omics analysis on the pathway level, pulmonary metabolomic pathway quantitative analytical results displayed that seven pathways were prominently regulated, meanwhile, which also contributed to the apparent visualization of three different groups. Similarly, analogous results were obtained from pathway quantitative analyses of fecal metabolomics and pulmonary transcriptomics (Fig. 6A). To explain the dynamic changes of gene expression and internal metabolism in response to the treatment, the correlative transcriptomic and metabolomic data was integrated for the underlying mechanism. As shown in Fig. 6B, AA Metabolism and Phospholipid Biosynthesis were all meaningfully correlated with Positive Regulation of Phosphatidylinositol (PI) 3 Kinase Signaling, Regulation of PI 3

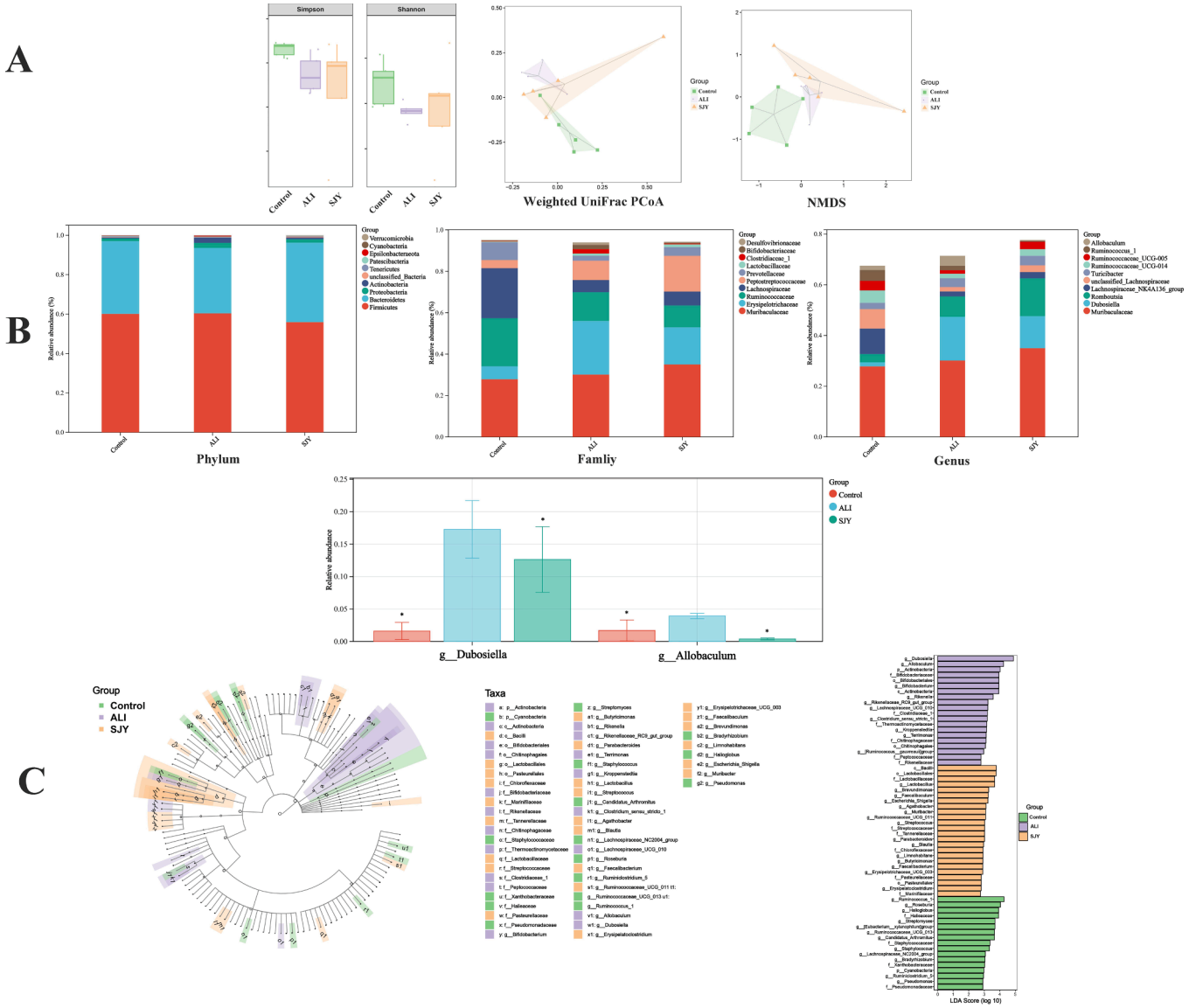

Fig. 5. The effects of SJY against ALI on gut microbial composition and structure. (A) The community function diversity (Shannon indices and Simpson indices), and Analysis of β diversity by Weighted UniFrac PCoA analysis of gut microbiota and non-metric multi-dimensional scaling (NMDS); (B) Dominant phyla, families and genera in each group; (C) The linear discriminant analysis effect size (LEfSe) analysis identified gut bacterial biomarkers in three groups of rats.

Kinase Signaling, PI 3 Kinase Signaling, Positive Regulation of Apoptotic Cell Clearance, Regulation of Apoptotic Cell Clearance and Apoptotic Cell Clearance. Considering the crucial role of AA metabolic dysregulation in inflammatory disorders (e.g., ALI), to further explore the potential crosstalk between AA metabolism and ALI pathogenesis, the correlation heatmap of AA metabolism and characteristic indicators of ALI in lung was reasonably obtained, that AA metabolic reprogramming was positively correlated with the levels of GSH and SOD; but negatively correlated with the levels of IL-3, IL-6, TNF-α and MDA (Fig. 6B). Interestingly, considering the correlogram of AA metabolic reprogramming and apoptosis related pathway in different groups, an exclusive significant correlation was attributed only to the state of ALI (Fig. 6B). For further mechanism exploration on the gut-microbiota-lung axis, data-mining from different bio-samples were deeply integrated on account of the correlation heatmap results of pulmonary AA metabolic pathway and fecal metabolic pathway, that five fecal pathways were obtained with noticeable correlations including biosynthesis of amino acids and methionine metabolism, etc. (Fig. 6C). Subsequently, the heatmap of integrative analysis between metabolic expression patterns and microbiomes in feces showed that eleven micro-floras were concerned with demonstrable correlations (Fig. 6C). For example, an obvious negative correlation was observed between g__*Ruminococcaceae*_UCG-011 and 2-oxocarboxylic acid metabolism.

4. Discussion

The first research objective of this study is to conduct a comprehensive component analysis of SJY from both *in vitro* and *in vivo* perspectives. Afterwards network pharmacology represented a crucial bridge between components in SJY and action targets/pathways of ALI. Additionally, the primary research highlight of our study is the systematic intervention mechanism exploration of SJY on ALI by employing a combined multi-omics approach for the first time, which included reprogramming of metabolic profile, regulation of characteristic gene levels and abatement of microbial dysbiosis, demonstrated that SJY might alleviate inflammatory cell infiltration and regulate the expression of cytokines, further regulate the crosstalk of metabolite-target-pathway-microflora, as well as associated bioprocesses, on the gut-microbiota-lung axis.

Considering the transferability of ingredients from *in vitro* to *in vivo* and the absorption of ingredients to exert beneficial intervention effects, the network pharmacological analysis on the basis of component analysis explained a clear modular topology consisting of the interaction network of SJY targets, anti-ALI targets, and associated pathways. Multi-components, such as rutin, chlorogenic acid, amygdalin, phillyrin, naringenin, acacetin and liquiritin, etc., might play intervention roles in ALI by regulating cytokine expression and modulating the PI3K-Akt signaling pathway, and endogenous metabolisms, etc. Moreover, the beneficial effects of potential active ingredients in SJY from the network against ALI have been supported, providing a reliable theoretical basis for the research and development of novel anti-inflammatory drugs in clinical practice (Abdallah et al., 2020, Wang et al., 2020). The potential therapeutic compounds might be used as leading markers for quality control, pharmacokinetic analysis and therapeutic drug monitoring for clinical use in real-world scenarios. The intricate ternary network of component-target-signaling, as a systemic biology-based methodology, objectively reflected the advantageous characteristics of TCM on systemic disorders, namely multi-component, multi-target and multi-pathway, appraising the intervention effects of SJY from the aspect of molecule to provide the interaction of TCM ingredients and action targets, and to further visualize the metabolic network regulation for therapy, thus conducive to the key targets/biomarkers identification from associated upstream/downstream signaling pathways.

As the final results of bio-processes, the combined LC-MS and ^{1}H NMR metabolomics were firstly carried out, based on the calculative metabolic disturbances from the network. Since the pathological state of the disease could be directly and sufficiently reflect by analyzing the samples of the lesion location, the lung homogenates were adopted for ALI metabolomics analyses. On the other hand, regarding the TCM theory of "exterior-interior interrelation of lung and large intestine" and considering the scientific role of intestinal flora as a crucial bridge between environment/disease status and host health (Lee et al., 2021). The fecal samples were also collected for thoroughgoing mechanism investigation.

First of all, LC-MS and ^{1}H NMR metabolomics were used considering their analytical complementarity. Unsurprisingly, almost no repetition (except L-proline) was gained for DMs from two techniques, which laterally reflected the desirability and availability for methodical combining. Then, from the perspective of instruments, a total of 177 DMs (including 76 for ESI^{+} and 101 for ESI^{-}) and 44 DMs were obtained for LC-MS and ^{1}H NMR, respectively. As shown in Table S5, it was worth mentioning that several endogenous compounds such as amino acids with poor performances in LC-MS were effectively identified by ^{1}H NMR due to high polarity. Next, from the perspective of bio-samples, the numbers of DMs in lung and feces were 146 and 75, respectively. Most types of endogenous compounds, especially AAs and lipids, were identified as pulmonary DMs, meanwhile, amino acids were accounted for the majority of endogenous composition in feces. Among them, Sarcosine, L-Cysteine, L-Serine, L-Proline, LPE(18:0), LPC(18:0), Glycolic acid, D-(-)-3-Phosphoglyceric acid and PE(P-16:0/22:6) were repeatedly tested in both two bio-samples. Taken together, a total of 221 different forms of DMs were screened out for ALI, among which 77 were down-regulated significantly and 144 were up-regulated prominently compared with control group, and most of them could be effectively intervened by SJY. Citrate has always been known as an important intermediate in the tricarboxylic acid cycle and was also an essential metabolite involved in various biological processes, implying its pivotal value in clinic. After SJY intervention, the markedly increased citrate level as a result of ALI modeling recovered significantly, which could be due to one of its important internal roles, namely as a key metabolite for macrophages in immune and inflammation regulation (Williams and O'Neill, 2018). Accompany with the fluctuation of redox and immune homeostasis, a significant decreasing generation of oxidized linoleic acid metabolites, particularly 9-HODEs, was observed in our ALI group, which could be related reasonably to the influence of lipoprotein-associated phospholipase A2 activity. The phospholipase A2, recognized as a specific clinical inflammatory marker, could generate lipid pro-inflammatory substances which in turn produce various lung injury events, including alveolar epithelial cell death and abnormal endothelial function, stimulating the production of adhesion factors and cytokines. These substances could further generate a self-reinforcing cycle by chemotactic inflammatory cells, producing more pro-inflammatory substances (Pecorelli et al., 2019). The levels of various lipids, especially phospholipids (such as PC, PE, LPC, etc.), were very sensitive to ALI modeling and SJY intervention, indicating one of the pivotal pathological features of ALI was the relationship between lipid metabolic disorder and OS/lipid peroxidation (Chen et al., 2022). The levels of 11-HETE, 19-HETE and AA, etc., (involved with AA metabolism) were significantly related to the pathological state in our results, which was in accordance with the identity of endogenous AAs and AA metabolism in inflammation/OS-related mechanisms (Zhang et al., 2022).

Given results of metabolomics were limited by a series of latent metabolites and relevant pathways as results of bio-processes without further exploration of their connected upstream targets as causes of bio-processes. More information about a more precise network of SJY against ALI was obtained by RNA-seq analysis to extensively characterize the entire gene expression profiles and functional changes from the perspective of complementarity. At last, a total of 263 DEGs (intervened by SJY) were suggested, which just verify and supplement the molecular mechanism results of network pharmacology on the gene level. Among them, the intersection genes of RNA-seq and network pharmacology were filtered as key targets, and recommended as the

next step researching focuses with validation by qRT-PCR (Fig. S4). Besides, the relationships between these targets with putative ALI related pathology have been reported. As a multifunctional cytokine, IL-10 participated in inflammatory and immune reactions, related to apoptosis/PI3K signaling, and was recognized as an inflammatory and immunosuppressive factor. IL-10 could not only affect the immune system, but also could affect many pathological and physiological processes by regulating growth factors and cytokines, playing an important role in the clinical diagnosis and treatment (Wang et al., 2021). Improving lipid metabolism and OS by modulating LCAT activity has been reported for targeted disease treatment (Yang et al., 2022). The correlation between CXCR2 with apoptosis/PI3K-Akt signaling pathway in disorders of inflammation/OS has been suggested (Sun et al., 2019; Cheng et al., 2021). Complement C5 was produced from complement activation and further cleaved to release C5a, initiating an adaptive immune response to release cytokines (TNF and IL-6, etc.). Excess C5a

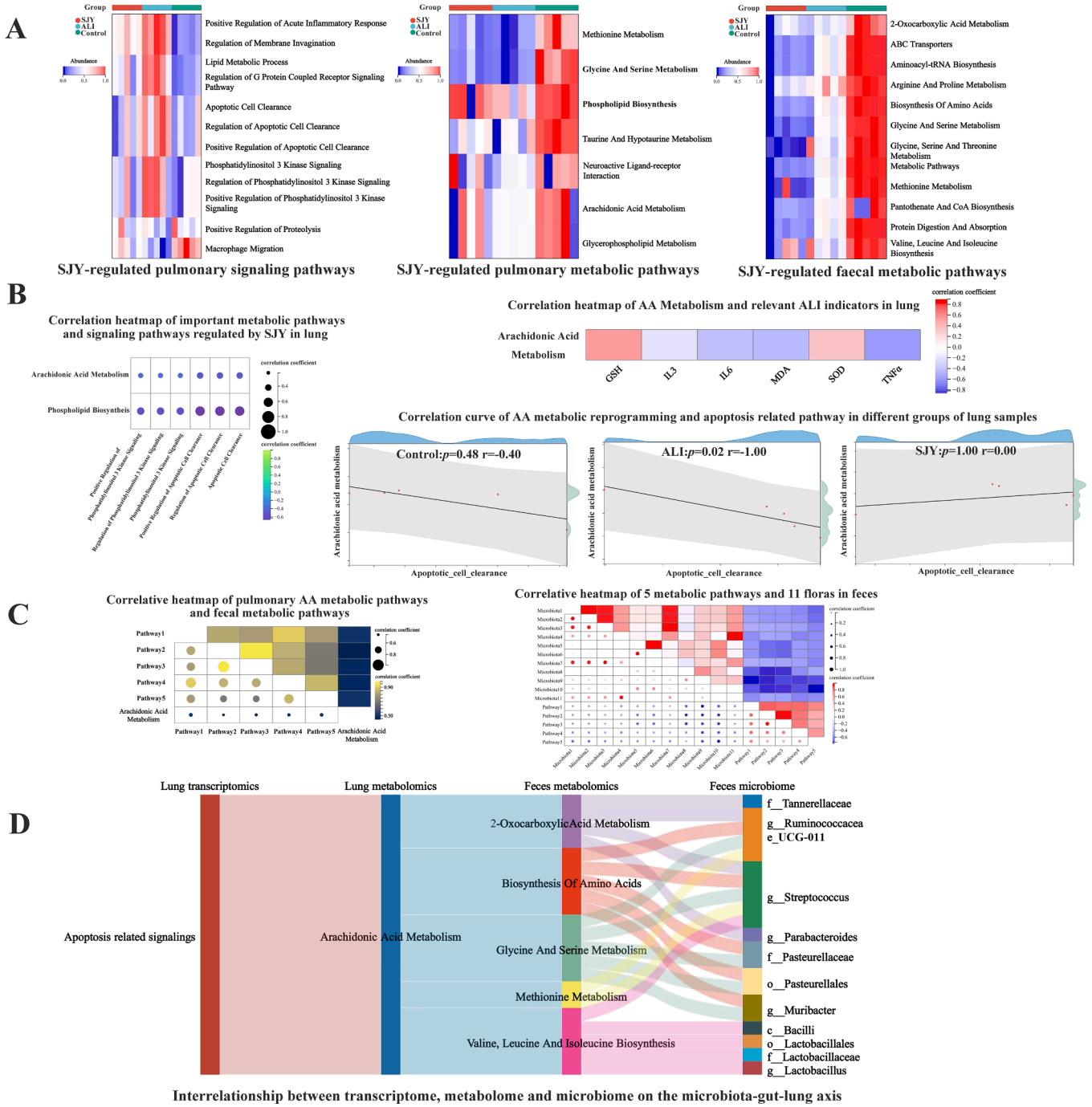

Fig. 6. Integrative multi-omics analysis of SJY against ALI. (A) Representative SJY-regulated pulmonary signaling pathways, pulmonary metabolic pathways and fecal metabolic pathways; (B) Correlation of important metabolic pathways and signaling pathways regulated by SJY in lung; (C) Correlative heatmap of pulmonary AA metabolic pathways and fecal metabolic pathways, and Correlative heatmap of 5 metabolic pathways and 11 floras in feces (Microbiota1, c__*Bacilli*. Microbiota2, o__*Lactobacillales*. Microbiota3, f__*Lactobacillaceae*. Microbiota4, f__*Tannerellaceae*. Microbiota5, f__*Pasteurellaceae*. Microbiota6, o__*Pasteurellales*. Microbiota7, g__*Lactobacillus*. Microbiota8, g__*Muribacter*. Microbiota9, g__*Ruminococcaceae*_UCG-011. Microbiota10, g__*Streptococcus*. Microbiota11, g__*Parabacteroides*. Pathway1, 2-Oxocarboxylic Acid Metabolism. Pathway2, Biosynthesis of Amino Acids. Pathway3, Glycine and Serine Metabolism. Pathway4, Methionine Metabolism. Pathway5, Valine, Leucine and Isoleucine Biosynthesis.); (D) Interrelationship between transcriptome, metabolome and microbiome on the microbiota-gut-lung axis.

could also stimulate neutrophils to generate ROS, inducing a wide variety of pro-inflammatory effects, including cytokine release and cell death by apoptosis (Carvelli et al., 2020). On the other hand, as action targets, the putative interactions of these key targets with SJY's ingredients (consistent with network pharmacology analysis results) were also verified and visualized via molecular docking to provide more evidences for the therapeutic effects of SJY against ALI (Fig. S4 and Table S7). Beyond the target level, the importance of PI3K-Akt, viral protein interaction with cytokine and cytokine receptor, etc. was further revealed with significance on the basis of our enrichment analysis results on the pathway level from the complex bio-system (Fig. 6).

Considering the identity of gut microbiota as important modulators of host-flora interaction on the gut-microbiota-lung axis, and regarding the role of microbiome dysbiosis in the pathogenesis of ALI, fecal samples were analyzed by 16S rRNA for deeper mechanism elucidation (Hashimoto et al., 2022). In this study, the relative abundances of several microfloras, including *Bacilli*, *Lactobacillales*, etc. were significantly different among different groups, implied the characteristic microbiota dysbiosis during ALI and the modulation effects of SJY. In concert, supported by other studies, the anti-inflammatory response has been attributed to *Lactobacillus* biofilms through influencing the secretion of macrophage-derived cytokines, such as the inhibition of pro-inflammatory TNF-α while the promotion of anti-inflammatory IL-10, reducing markers of inflammation and apoptosis induced by LPS (Dias et al., 2021). Studies have revealed that *Streptococcus* could release inflammatory components (such as peptidoglycan and hydrogen peroxide) during pulmonary inflammation to further trigger inflammation by means of multiple inflammatory cascades (such as chemokine/cytokine cascade, the complement cascade, etc.), thus mediating the release of pro-inflammatory factors, e.g., IL-6 and TNF, modulating Nod receptor activation, etc. Nonetheless, the metabolism of *Streptococcus* could produce hydrogen peroxide to cause apoptosis and tissues injuries. Additionally, the activation of complement pathways could contribute to the release of the chemoattractant IL-10, leading to neutrophil recruitment and contributing to the host response pathology. Additionally, the complement could not only contribute to bacteria opsonization but also contribute to forming membrane attack complex (under the action of C5) (Loughran et al., 2019). On the other hand, serious inflammation injuries involved with *Streptococcus* in the cells and tissues have been reported to be significantly regulated by taurine, which could inhibit Akt/mTOR signaling, activate autophagy and suppress NF-κB pathway over-activation, etc. (Wang et al., 2021).

Considering above-mentioned crosstalk of metabolites, targets, pathways and bio-processes, comprehensively datamining by integrative multi-omics analyses were carried out to further explore the molecular mechanism from various complementary levels. First, focusing on SJY's effects on lesion tissue lung, correlation analysis of metabolomics and transcriptomics were further integrated on the pathway level (Fig. 6). Several worthwhile relationships were observed, namely AA metabolism with apoptosis related signaling pathways, AA metabolism with PI3K-Akt related signaling pathways, etc. The association between lipid peroxidation of biomarkers (such as AA, etc.) and certain lipid peroxidation relevant procedures (e.g., PI3K-Akt, etc.) has been mentioned. Besides, the PI3K-Akt pathway and its related regulatory factors, such as pro-apoptotic proteins and caspase cascades, were involved in the entire course of ALI, such as early inflammatory response, pulmonary edema, and later tissue repair, airway remodeling, and emphysema, which are of great significance for clinical diagnosis and treatment (Zhao et al., 2022). Related literature also has reported the possible association between AA metabolic reprogramming with apoptosis (Yang et al., 2021). Besides, apoptosis was reported to be induced by apigenin through inhibition of PI3K-Akt pathway (Yang et al., 2018). Hence, the pulmonary AA metabolic reprogramming attracted our attention. Accordingly, the obvious correlation between pulmonary AA metabolic profile and ELISA indicators (inflammation and OS) made us more interested in pulmonary AA reprogramming and its relation to apoptosis (Fig. 6), which could be applied as the guider to further explore the complex molecular mechanism. Most interestingly, the correlogram of AA metabolic reprogramming and apoptosis related pathway in different groups was further acquired with an exclusive significant correlation attributed only to the state of ALI (Fig. 6), which supported the hypothesis of the key role of the crosstalk of AA metabolic reprogramming and apoptosis to a certain degree. Those results provided the possibility for the treatment of ALI by specifically intervening in AA metabolism and apoptosis, which could also promote the promotion of SJY clinically.

As mentioned before, considering the importance of the two types of bio-samples (lung and feces on the gut-microbiota-lung axis) for in-depth mechanism research, further mining was carried out from the association of lung-feces data and the interaction of metabolomics-microbiomes information, guided by the key indicator (pulmonary AA metabolic reprogramming). A total of five pathways in feces (including biosynthesis of amino acids, and so on) were screened out with significance from the correlation heatmap of metabolic pathways (with pulmonary data) (Fig. 6). Except for AA metabolism, the dysregulation of amino acids was also another sign of ALI with the clinical significance that changing the metabolism of certain amino acids might influence the levels of both inflammatory cell and inflammatory factors, and might interfere the recovery from pulmonary injuries. Based on these five fecal metabolic pathways, considering the characteristic variation of gut bacterial richness has typically been a common hallmark for the specific disease (Lu et al., 2022), the intervention effects of SJY on ALI were further discussed on the microflora level based on the correlation between metabolic pathways and microflora. Notably, eleven floras were markedly screened out (Fig. 6), among which, linkages were also observed, for example, both genus *Streptococcus*. and genus *Lactobacillus* were associated to order *Lactobacillales* and class *Bacilli*, suggesting meaningful interactions and features for specific floras. Additionally, studies have supported the role of these characteristic microflora in disease therapy, for example, the abundance of *Lactobacillus* at the genus level could be influenced by drug therapy (Li et al., 2022).

In summary, our study investigated the intervention mechanism of SJY on ALI at the level of compound, target, pathway as well as network. The multi-omics information was combined and interpreted to discuss consistent conclusions from various biosystems that SJY may alleviate ALI by intervening the crosstalk of AA-apoptosis-microflora on the gut-microbiota-lung axis (Fig. 6). However, the mechanism of further internal interactions has not yet been explored. It's still unclear about the detailed regulatory mechanism of SJY on the relationship between pulmonary AA metabolism and apoptosis, and how much the feces reflected the pathological state in real time during SJY's intervention on ALI. It's necessary to carry out in-depth mechanism research focusing on key variables (such as floras, targets and pathways, etc.) with multiple SJY administration dosages and positive control to further screen out the core variables by upregulating or downregulating the variables that need to be tested. Moreover, on the basis of the core variables accounting for the anti-ALI effects of SJY, the material basis relating to the action mechanism is also required to be ulteriorly screened out, under the correlation between quantity and effect. Considering the modes and sites of action between compounds in SJY and targets of ALI were still unclear, further experiments (such as the detection of interactions between chemical compound and protein, detection of protein binding sites using mass spectrometry, etc.) should be investigated.

5. Conclusion

In conclusion, our research explored the efficacy of SJY for the treatment of ALI and revealed the in-depth intervention mechanism by systematically integrating multiple techniques. Overall, we combined component analysis, network pharmacology, metabolomics (LC-MS/MS and ^{1}H NMR), RNA-sequencing and 16S rRNA gene sequencing to elucidate that SJY could alleviate ALI by regulating the gut-microbiota-

lung axis through modulating the disturbance of AA metabolic reprogramming-apoptosis related pathways in lung and endogenous metabolites-microflora composition in feces, as well as their associations, providing a novel paradigm to explore the potential mechanism of TCM on diseases.

CRediT authorship contribution statement

Song Lin: Writing – original draft, Methodology, Formal analysis. **Ruinan Ren:** Software, Formal analysis. **Fang Wang:** Software, Formal analysis. **Zilong He:** Investigation, Formal analysis. **Cuiyan Han:** Writing – review & editing, Supervision. **Jinling Zhang:** Investigation, Data curation, Visualization. **Wenbao Wang:** Validation. **Jie Zhang:** Validation. **Huiyu Wang:** Visualization. **Huimin Sui:** Visualization. **Tianyang Wang:** Conceptualization, Writing – review & editing, Supervision, Project administration, Funding acquisition.

Data availability

Data will be made available on request.

Acknowledgments

Thanks to Shanghai Bioprofile Technology CO., Ltd (Shanghai, China). for the extraction of RNA and DNA, as well as the sequencing of RNA and 16S rRNA.

Authors' contributions

Song Lin, Tianyang Wang and Zilong He designed and carried out the *in vivo* experiment. Song Lin, Ruinan Ren and Fang Wang carried out the *in vitro* experiment. Jinling Zhang, Wenbao Wang and Jie Zhang helped to develop the method for measurement and analyzed the data. Song Lin, Tianyang Wang, Huimin Sui and Huiyu Wang contributed to the preparation of the figures. Song Lin, Tianyang Wang and Cuiyan Han designed the study and drafted the manuscript. All authors have read and approved the final version of the manuscript. All data were generated in-house, and no paper mill was used. All authors agree to be accountable for all aspects of work ensuring integrity and accuracy.

Funding

This work was supported by Heilongjiang Provincial Natural Science Foundation of China (LH2021H124), Science and Technology Bureau of Qiqihar (LHYD-2021011), and Research Institute of Medicine & Pharmacy of Qiqihar Medical University (QMSI2021B-03, 2022-ZDPY-004, 2023-ZDPY-001, QMSI2023E-01).

Appendix A. Supplementary material

Supplementary data to this article can be found online at https://doi.org/10.1016/j.arabjc.2024.105646.

References

Abdallah, H.M., El-Agamy, D.S., Ibrahim, S.R.M., et al., 2020. Euphorbia cuneata represses LPS-induced acute lung injury in mice via its antioxidative and anti-inflammatory activities. Plants (Basel) 9, 1620. https://doi.org/10.3390/plants9111620.

Carvelli, J., Demaria, O., Vély, F., et al., 2020. Association of COVID-19 inflammation with activation of the C5a–C5aR1 axis. Nature 588, 146–150. https://doi.org/10.1038/s41586-020-2600-6.

Chen, Z., Han, S., Zheng, P., et al., 2022b. Landscape of lipidomic metabolites in gut-liver axis of Sprague-Dawley rats after oral exposure to titanium dioxide nanoparticles. Part. Fibre Toxicol. 19, 53. https://doi.org/10.1186/s12989-022-00484-9.

Chen, Y., Peng, M., Li, W., et al., 2022a. Inhibition of inflammasome activation via sphingolipid pathway in acute lung injury by Huanglian Jiedu decoction: an integrative pharmacology approach. Phytomedicine 107, 154469. https://doi.org/10.1016/j.phymed.2022.154469.

Cheng, Y., Mo, F., Li, Q., et al., 2021. Targeting CXCR2 inhibits the progression of lung cancer and promotes therapeutic effect of cisplatin. Mol. Cancer 20, 62. https://doi.org/10.1186/s12943-021-01355-1.

Dias, A.M.M., Douhard, R., Hermetet, F., et al., 2021. Lactobacillus stress protein GroEL prevents colonic inflammation. J. Gastroenterol. 56, 442–455. https://doi.org/10.1007/s00535-021-01774-3.

Hashimoto, Y., Eguchi, A., Wei, Y., et al., 2022. Antibiotic-induced microbiome depletion improves LPS-induced acute lung injury via gut-lung axis. Life Sci. 307, 120885 https://doi.org/10.1016/j.lfs.2022.120885.

Lee, D.Y.W., Li, Q.Y., Liu, J., et al., 2021. Traditional Chinese herbal medicine at the forefront battle against COVID-19: Clinical experience and scientific basis. Phytomedicine 80, 153337. https://doi.org/10.1016/j.phymed.2020.153337.

Li, Y., Liu, C., Luo, J., et al., 2022. Ershiwuwei Lvxue Pill alleviates rheumatoid arthritis by different pathways and produces changes in the gut microbiota. Phytomedicine 107, 154462. https://doi.org/10.1016/j.phymed.2022.154462.

Liu, S., Yin, R., Yang, Z., et al., 2022. The effects of rhein on D-GalN/LPS-induced acute liver injury in mice: results from gut microbiome-metabolomics and host transcriptome analysis. Front. Immunol. 13, 971409 https://doi.org/10.3389/fimmu.2022.971409.

Loughran, A.J., Orihuela, C.J., Tuomanen, E.I., 2019. Streptococcus pneumoniae: invasion and Inflammation. Microbiol Spectr. 7 https://doi.org/10.1128/microbiolspec.GPP3-0004-2018.

Lu, Y., Yuan, X., Wang, M., et al., 2022. Gut microbiota influence immunotherapy responses: mechanisms and therapeutic strategies. J. Hematol. Oncol. 15, 47. https://doi.org/10.1186/s13045-022-01273-9.

Pecorelli, A., Cervellati, C., Cordone, V., et al., 2019. 13-HODE, 9-HODE and ALOX15 as potential players in Rett syndrome OxInflammation. Free Radic. Biol. Med. 134, 598–603. https://doi.org/10.1016/j.freeradbiomed.2019.02.007.

Shen, J., 2020. Analysis of clinical prescriptions and symptoms of Sangju Yin. China's Naturopathy. 28, 102–104. 10.19621/j.cnki.11-3555/r.2020.0852.

Sun, F., Wang, J., Sun, Q., et al., 2019. Interleukin-8 promotes integrin β3 upregulation and cell invasion through PI3K/Akt pathway in hepatocellular carcinoma. J. Exp. Clin. Cancer Res. 38, 449. https://doi.org/10.1186/s13046-019-1455-x.

Wang, Z., Lan, R., Xu, Y., et al., 2021b. Taurine alleviates *Streptococcus uberis*-induced inflammation by activating autophagy in mammary epithelial cells. Front. Immunol. 12, 631113 https://doi.org/10.3389/fimmu.2021.631113.

Wang, T., Lin, S., Li, H., et al., 2020a. A stepwise integrated multi-system to screen quality markers of Chinese classic prescription Qingzao Jiufei decoction on the treatment of acute lung injury by combining 'network pharmacology-metabolomics-PK/PD modeling'. Phytomedicine 78, 153313. https://doi.org/10.1016/j.phymed.2020.153313.

Wang, T., Lin, S., Liu, R., et al., 2020b. Acute lung injury therapeutic mechanism exploration for Chinese classic prescription Qingzao Jiufei Decoction by UFLC-MS/MS quantification of bile acids, fatty acids and eicosanoids in rats. J. Pharm. Biomed. Anal. 189, 113463 https://doi.org/10.1016/j.jpba.2020.113463.

Wang, T., Lin, S., Liu, R., et al., 2020c. Metabolomic profile perturbations of serum, lung, bronchoalveolar lavage fluid, spleen and feces in LPS-induced acute lung injury rats based on HPLC-ESI-QTOF-MS. Anal. Bioanal. Chem. 415, 1215–1234. https://doi.org/10.1007/s00216-019-02357-1.

Wang, T., Li, P., Meng, X., et al., 2022. An integrated pathological research for precise diagnosis of schizophrenia combining LC-MS/(1)H NMR metabolomics and transcriptomics. Clin. Chim. Acta 524, 84–95. https://doi.org/10.1016/j.cca.2021.11.028.

Wang, J.F., Wang, Y.P., Xie, J., et al., 2021a. Upregulated PD-L1 delays human neutrophil apoptosis and promotes lung injury in an experimental mouse model of sepsis. Blood 138, 806–810. https://doi.org/10.1182/blood.2020009417.

Williams, N.C., O'Neill, L.A.J., 2018. A Role for the Krebs cycle intermediate citrate in metabolic reprogramming in innate immunity and inflammation. Front. Immunol. 9, 141 https://doi.org/10.3389/fimmu.2018.00141.

Wu, Y.Z., Zhang, Q., Wei, X.H., et al., 2022. Multiple anti-inflammatory mechanisms of Zedoary Turmeric Oil Injection against lipopolysaccharides-induced acute lung injury in rats elucidated by network pharmacology combined with transcriptomics. Phytomedicine 106, 154418. https://doi.org/10.1016/j.phymed.2022.154418.

Wypych, T.P., Wickramasinghe, L.C., Marsland, B.J., 2019. The influence of the microbiome on respiratory health. Nat. Immunol. 20, 1279–1290. https://doi.org/10.1038/s41590-019-0451-9.

Yang, J., Pi, C., Wang, G., 2018. Inhibition of PI3K/Akt/mTOR pathway by apigenin induces apoptosis and autophagy in hepatocellular carcinoma cells. Biomed. Pharmacother. 103, 699–707. https://doi.org/10.1016/j.biopha.2018.04.072.

Yang, J., Li, S., He, L., et al., 2021. Adipose-derived stem cells inhibit dermal fibroblast growth and induce apoptosis in keloids through the arachidonic acid-derived cyclooxygenase-2/prostaglandin E2 cascade by paracrine. Burns Trauma 9, tkab020. https://doi.org/10.1093/burnst/tkab020.

Yang, K., Wang, J., Xiang, H., et al., 2022. LCAT- targeted therapies: progress, failures and future. Biomed. Pharmacother. 147, 112677 https://doi.org/10.1016/j.biopha.2022.112677.

Zhang, T., Yang, S., Zhang, J., 2014. Sangjuyin attenuates acute lung injury induced by lipopolysaccharide in mice. Pharmacol. Clin. Chin. Mater. Med. 30, 12–14. https://doi.org/10.13412/j.cnki.zyyl.2014.05.004.

Zhang, J., Zhang, M., Zhang, W.H., et al., 2022. Total flavonoids of Inula japonica alleviated the inflammatory response and oxidative stress in LPS-induced acute lung injury via inhibiting the sEH activity: insights from lipid metabolomics. Phytomedicine 107, 154380.

Zhao, Y., Nogueira, M.S., Milne, G.L., et al., 2022. Association between lipid peroxidation biomarkers and microRNA expression profiles. Redox Biol. 58, 102531 https://doi.org/10.1016/j.redox.2022.102531.